Scan-by-Scan Averaging and Adjacent Detection Merging to improve Ship Detection in HFSWR

J. O. Hinz, M. Holters, U. Zölzer

Department of Signal Processing and Communications
Helmut Schmidt University, Holstenhofweg 85, 22043 Hamburg, Germany
jan.hinz@hsu-hh.de

***Abstract*—High Frequency Surface Wave Radars (HFSWRs) play an important role in long-range ocean surveillance, with particular interest in reliable detection and tracking of far-distant ships. One of the biggest challenges in ship target detection in HFSWR is the non-homogeneous detection background. Depending on the chosen detection parameters, this non-homogeneous detection background leads to extensive false alarms or poor detection performance.**

This paper shows how scan-by-scan averaging can help to reduce a significant number of these false alarms. In addition the problem of target spreading and multiple detections of the same target is addressed by an Adjacent Detection Merging Algorithm (ADMA). Furthermore, it is shown how the result of the ADMA can be used to improve the estimation of target parameters, such as azimuth, Doppler and range.

I. Introduction

Typical tasks of High Frequency Surface Wave Radars (HFSWRs) are ocean state monitoring and target detection up to ranges of 200 km. Of particular interest is the detection of ships, which, due to the non-homogeneous detection background, is a difficult task. The detection background is mainly dominated by two regions: the external noise dominated region and sea-clutter dominated region.

The most used type of target detectors in HFSWR are the group of 1D/2D/3D Constant False Alarm Rate (CFAR) algorithms, which decide about the presence of a target, based on neighboring reference cells in azimuth, Doppler and range (ADR).

What has not been analyzed in the context of HFSWR is the relationship between the CFAR algorithm, the coarse HFSWR resolution and typical ship target movements. This analysis is described in Sec. II. Based on the analysis, in Sec. III, we present our scan-by-scan averaging approach to reduce the number of false alarms. In addition we address the problem of multiple detections of the same target via an Adjacent Detection Merging Algorithm (ADMA), followed by a target parameter estimation (TPE). In Section IV the results of the proposed approach are presented. In the end the paper is summarized with a conclusion in Sec. V.

TABLE I
Typical resolution capabilities of a HFSWR

	Equation	Typical values
range resolution	$\Delta r = c/(2 \cdot B)$	$\Delta r \geq 1500\,\mathrm{m}$
Doppler resolution	$\Delta f_D = 1/(N_s \cdot T_s)$	$\Delta f_D \geq 0.0075\,\mathrm{Hz}$
azimuth resolution	$\Delta\theta \approx 102^\circ/M$	$\Delta\theta \geq 6.38^\circ$

II. HFSWR and ship target movements

A. Resolution of HFSWRs

HFSWRs can be seen different from typical microwave radars due to their coarse range and azimuth resolution. In the following we will present typical values for an HFSWR Frequency Modulated Continuous Wave (FMCW) radar in terms of range, Doppler and azimuth resolution. The range resolution is given by

$$\Delta r = c/(2 \cdot B), \tag{1}$$

in which c denotes the speed of light and B the bandwidth of the FMCW signal. The Doppler resolution is defined by

$$\Delta f_D = 1/(N_s \cdot T_s), \tag{2}$$

which is the inverse of the coherent integration time (CIT), which itself is the product of the number of sweeps N_s in each CIT and the time duration of each sweep T_s [1]. The azimuth resolution for a radar with a phased array antenna is defined by its Half Power Beamwidth (HPBW), which can be approximated by

$$\Delta\theta \approx 102^\circ/M, \tag{3}$$

assuming an M element array with isotropic elements and an inter element spacing of half of the radar operating wavelength [2]. With a bandwidth B of 100 kHz, the CIT formed by $N_s = 512$ and $T_s = 0.26\,\mathrm{s}$ and $M = 16$ antenna elements this leads to the typical HFSWR resolution values enlisted in Table I.

The coarse range resolution can be explained by the strong frequency occupancy of HF spectrum and a very limited available consecutive bandwidth of less than 100 kHz. The

978-1-4673-2393-2/12/$31.00

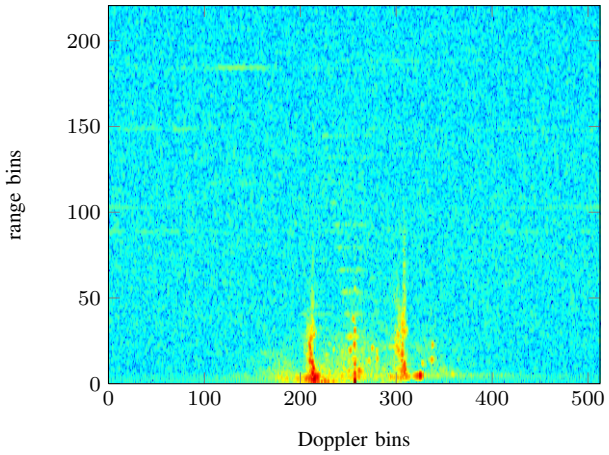

Fig. 1. Typical range-Doppler map

coarse azimuth resolution is a consequence of the limited length of the receiver antenna array. This limitation can be caused by geographical or economic constraints of the occupied property, with typical array lengths in between 75 and 750 meters. Colocated Multiple-Input Multiple-Output (MIMO) radar approaches can help to reduce these constraints and build a compact array with improved azimuth resolution [3].

Due to the long CIT of HFSWRs (up to 180 s), the Doppler resolution is very accurate. Increasing the CIT will lead to an increased Doppler resolution, but at the same time will pose further requirements on the target movement and the stationarity of the detection background. To obtain an optimal detection performance, it is typically assumed that during the CIT the potential target does not maneuver. In this case the target moves with a constant radial speed and is seen by the radar with a constant Doppler frequency. The strictness of this requirement can be illustrated by converting the Doppler resolution into a radial speed resolution via

$$\Delta v_r = -(\Delta f_D \cdot c)/(2 \cdot f_c), \tag{4}$$

in which f_c denotes the radar operating frequency. With a radar operating frequency f_c of 12.27 MHz this leads to a radial speed resolution Δv_r of less than 0.1 m/s. If a target's radial speed deviates more than one resolution cell Δv_r, the energy of the target will spread in adjacent resolution cells and the probability of detecting the target is reduced.

B. Target Detection in HFSWRs

Target detection in HFSWRs is typically carried out by the group of 1D/2D/3D CFAR algorithms. In case a 2D detection is used, the input to the detection is the well known range-Doppler map, with an example illustrated in Fig. 1.

The CFAR algorithm iteratively compares each Cell Under Test (CUT) to a threshold S defined by

$$S = T \cdot Z, \tag{5}$$

which is composed of a local power estimate Z of its neighboring range and Doppler cells and a constant scale factor T. The local reference power Z is determined according to the selected type of CFAR algorithm as presented in [4] with the constant scale factor T needed to make sure a chosen design false alarm rate P_{fa} is maintained.

Typically, several assumptions about the reference cells are made: 1.) The cells are independent and identically distributed (i.i.d.) and their family of probability density functions (pdfs) is known. 2.) The reference cells are free of interfering targets and only contain noise or clutter. 3.) The used guard cells make sure that the reference cells are free of target spreading.

If a square-law detector is used, the surrounding noise cells are typically modeled by the family of exponential distributions. In this case the T factor for the Cell-Averaging (CA)-CFAR can be calculated according to

$$T = P_{\text{fa}}^{-\frac{1}{N}} - 1, \tag{6}$$

in which N denotes the total number of reference cells and P_{fa} is the design false alarm rate [4].

For HFSWRs the choice of the number of reference cells in each dimension is a difficult task. It is a trade-off between these two cases: 1.) The usage of many cells (e.g. 20 cells in each dimension) provides accurate mean level estimates if above mentioned assumptions hold. In any case, increasing the number of reference cells also increases the probability that at least one of above assumptions is violated. 2.) The usage of few reference cells (e.g. four cells in each dimension) will provide less accurate mean level estimates, lead to a high T factor, but reduce the risk of violating the above mentioned assumptions.

Due to the non-homogeneous HFSWR detection background (a mixture of external noise and sea clutter) and using a fixed number of reference cells on the whole range-Doppler map, it is clear that the first case will likely result in extensive false alarms or missed detection [5]. Based on our experience we have obtained good results for four to eight reference cells in each dimension and two guard cells on each side of the CUT.

To avoid the problem of a non-homogeneous detection background, other types of radars, for example air surveillance radars, use an approach called clutter map (CM)-CFAR [6]. This approach compares the value of the current CUT (azimuth, range) to a threshold formed by previous scans of the same cell. Depending on whether the level in the CUT is above or below the threshold a target is declared or not.

If one transforms that idea to the HFSWR domain this implies that the detection in one particular range-Doppler cell is made by the values in the previous scans. Assuming a slow and non-maneuvering target with resolution cell sizes defined in Table I an effect called target-masking will occur: The threshold is sequentially raised until a potential target is not detected anymore.

C. Analysis of ship target movements

By analyzing the target movements of numerous medium to large ships by the use of Automatic Identification System (AIS) data we can conclude the following:

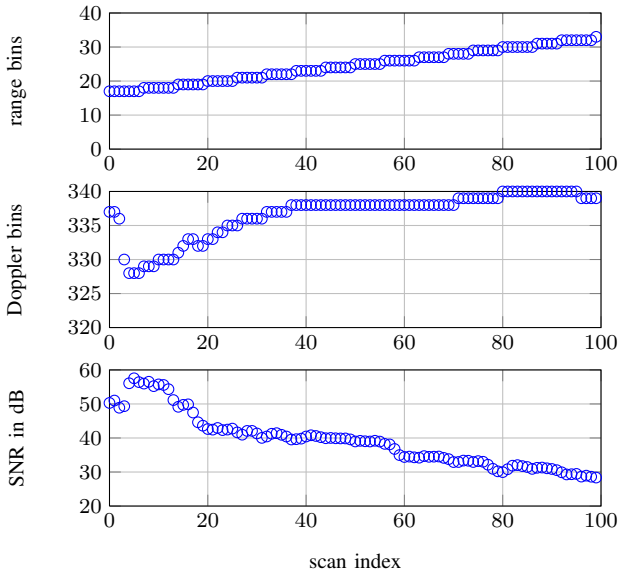

Fig. 2. Typical Ship Target movement - as seen by the radar

- The maximum cruising speed on the open sea is around 10 m/s, with economic cruising typically below 5 m/s.
- Under normal conditions ships keep the same course for quite some time (at least five to ten minutes).
- During this period ships prefer to move at constant speed, with no strong intentional de-/ or acceleration.

As the typical role of HFSWRs is long-range surveillance with ranges up to 200 km, the large size of a single resolution cell will lead to the fact that even fast targets will be located in the same range bin and beam for at least a couple of scans. In addition the maneuvering capabilities of medium to large ships is very limited. Thus, if a ship is not currently changing its course the Doppler component can be assumed to be fairly constant. This is in contrast to high-resolution radars used in the automotive or airborne domain, in which maneuvers are frequent and unavoidable.

An example of a typical ship movement, as measured by the radar, is illustrated in Fig. 2, in which the respective range and Doppler bin positions have been calculated from AIS data. In the presented case the target is moving at a fairly constant speed radially away from the radar. The whole period illustrated in Fig. 2 spans approximately one hour of measurement time, in which each time index corresponds to one CIT (also denoted as scan) of 133.12 seconds. Due to the overlapping processing of the CITs the time difference between two scan indexes is 33.28 seconds. At each scan the respective range and Doppler bins of the target as well as the corresponding Signal-to-Noise (SNR) ratio with respect to the external noise floor are shown.

Even though the target is moving, the coarse range resolution of HFSWRs leads to the fact that the target is located in the same range cell for some subsequent scans. If one neglects the first 25 scans of the second plot, a similar behavior can also be seen in terms of Doppler bins. At the same time it also justifies why increasing the CIT is not an option.

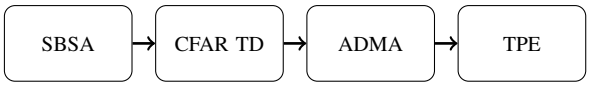

Fig. 3. Proposed Method - Overview

The last part of Fig. 2 shows the SNR of the target cell to the average external background as measured by the radar. Ignoring the negative trend of SNR due to the range dependent attenuation, this plot tells us something about the Radar Cross Section (RCS) fluctuations. The SNR is fairly constant (even up to 20 scans), if one neglect effects due to maneuvering as encountered during the first 25 scans. The small local changes in SNR can be attributed to the processing loss and can be influenced by the choice of the window functions.

III. Proposed Methods

The proposed scan-by-scan averaging (SBSA) method makes use of the particular combination of the coarse HFSWR range and azimuth resolution as well as the slow and only occasionally maneuvering ship targets. In addition we propose an efficient Adjacent Detection Merging Algorithm (ADMA) to eliminate several detections from the same target. Based on the output of the ADMA a target parameter estimation (TPE) is carried out. An overview of the proposed methods, including the task of target detection (TD), is visualized in Fig. 3.

A. Scan-by-Scan Averaging (SBSA)

As already stated before, a major limitation of TD in HFSWR is the limited number of usable reference cells due to clutter edges or interfering targets. Even applying CFAR algorithms with small reference windows usually lead to higher number of false alarms as intended by the design false alarm rate P_{fa} used in (6). This is partly due to the non-homogeneous background and partly due to several detections of the same target due to target spreading.

Our proposed method is to apply a scan-by-scan averaging filter to integrate the power of each range Doppler cell over of a number of subsequent scans. This can be carried out by a Finite Impulse Response (FIR) or an Infinite Impulse Response (IIR) filter, with the FIR filter equation defined by

$$p_{\mathrm{a,d,r}}[k] = \sum_{i=0}^{m-1} b[i] \cdot c_{\mathrm{a,d,r}}[k-i], \tag{7}$$

in which $c_{\mathrm{a,d,r}}[k]$ denotes the power at scan index k for one particular azimuth (a), Doppler (d) and range (r) cell. The FIR filter coefficients are denoted by $b[i]$ and m is the chosen number of integrated scans, commonly denoted as filter length. The adapted IIR filter equation is defined by

$$p_{\mathrm{a,d,r}}[k] = \sum_{i=0}^{m-1} b[i] \cdot c_{\mathrm{a,d,r}}[k-i] + \sum_{j=1}^{k} a[j] \cdot p_{\mathrm{a,d,r}}[k-j], \tag{8}$$

in which $a[j]$ are the feedback IIR filter coefficients. In both cases the filtering operation has to be carried out for each azimuth (a), Doppler (d) and range (r) cell.

TABLE II
TIME OF TARGET IN ONE RANGE CELL (RANGE RESOLUTION 1500 M)

Doppler bin	1	...	64	...	128
Doppler frequency [Hz]	0.075	...	0.4804	...	0.9615
radial speed [m/s]	0.09	...	5.87	...	11.74
time to cross cell [s]	16349	...	255.46	...	127.73
time in scans periods	488.26	...	4.67	...	0.83

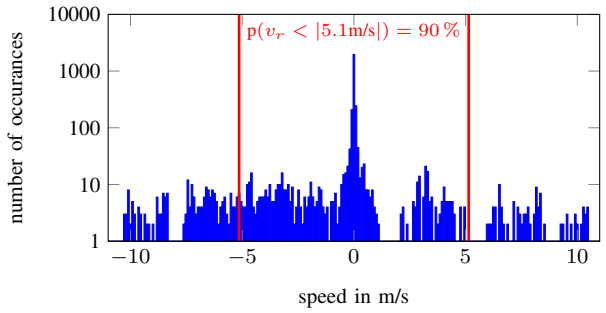

Fig. 4. Histogram of ship radial speeds - based on AIS data

The scan-by-scan averaging approach relies on the fact that the target (in our case a ship target) stays within the same range bin for at least a couple of scans and changes in beam number or Doppler bin can be neglected. Since HFSWRs are designed for wide-range surveillance, having coarse range and azimuth resolution these conditions are almost certainly fulfilled.

To estimate the number of scans a target is located in the same range cell (and thus to determine the filter parameter m and k) Table II is presented.

The table shows the positive Doppler bins 1, 64 and 128 resulting from a 512-point Doppler transform [7]. In addition the Doppler bin center frequencies as well as the resulting radial speeds are shown. The used parameters for the calculation are $f_c = 12.27\,\text{MHz}$, $B = 100\,\text{kHz}$, a CIT of $133.12\,\text{s}$ with 3/4 overlap and a 512-point FFT. For convenience only positive bins are shown and potential signs have been dropped. Furthermore, Table II shows us that a radially approaching/receding target with an economic speed of $5.87\,\text{m/s}$ and a radar with a range resolution of 1500 meters is situated 4.67 scans in the same range bin. A radial speed of $11.74\,\text{m/s}$ is given as a comparison but seldom encountered in practice. Figure 4 is the result of the evaluation of one hour of AIS data and shows the distribution of the monitored ships radial speed components.

It shows that $90\,\%$ of all AIS contacts have an absolute radial speed (relative to the radar) of less than $5.1\,\text{m/s}$.

B. Adjacent Detection Merging Algorithm (ADMA)

Another important aspect in HFSWR is target spreading, which is a result of the finite resolution in azimuth, Doppler and range. This can lead to the fact that a single target is detected several times in adjacent range and Doppler bins as well as beams.

Simply increasing the CFAR detection threshold by adapting the design false alarm rate in (6) cannot solve this problem since smaller targets would then remain undetected. Forwarding all detections, including several of the same target, could lead to a saturation of the tracking system, since significantly more tracks would have to be maintained.

This can be solved by the use of ADMA algorithms (also known as Plot Extractor or Hit Processors) [8] which cluster adjacent detections from the same target into a final hit without merging detections from two adjacent but independent targets. Surprisingly, although there are several publications about detection and tracking in HFSWR [9] [10], there is not much literature about ADMA in the context of HFSWR.

We see ADMA, together with the following target parameter estimation, as an additional processing step between conventional CFAR detection and tracking. ADMA can be used to form detection clusters, which then can be used as input parameters to the TPE of azimuth, Doppler and range. Besides the correct clustering of detections to hits, three problematic cases can occur, such as:

1) Two or more targets are merged into one hit.
2) Several adjacent noise/clutter detections are merged.
3) Noise/clutter detections adjacent to a target detection are merged into a hit.

Since targets are usually sparsely distributed in the ADR domain, the first case is not likely to occur. The second case is not a major problem since it helps us in keeping the number of false alarms low. The most relevant case is in which several noise/clutter detections are combined with one or several target detections. Depending on the ratio of false detections to corrected detections as well as their relative power an error in the TPE will occur.

We propose to use Connected Component Labeling (CCL), an algorithm widespread in computer vision concerned with the detection of connected regions in binary or grayscale images. In the simplest case the algorithm works on a binary image and iteratively compares each pixel to the local neighborhood, with common neighborhood metric being the 4-connectivity or 8-connectivity. Depending on if the current pixel is found to be part of any of its neighbor regions it is assigned an own label or assigned a label of one of its neighbors. More details can be found in [11].

To apply the CCL to the adjacent detection problem in HFSWR the detection list from the CFAR detection is converted into a binary ADR detection cube according to

$$l_{\text{a,d,r}}[k] = \begin{cases} 0 & \text{for } c_{\text{a,d,r}}[k] < S_{\text{a,d,r}}[k] \\ 1 & \text{for } c_{\text{a,d,r}}[k] \geq S_{\text{a,d,r}}[k], \end{cases} \tag{9}$$

in which $S_{\text{a,d,r}}[k]$ is the CFAR threshold according to (5). At the output of the CCL algorithm each hit h_u can be described by a set of detections in the ADR domain according to

$$h_u = \{(a_{u1}, d_{u1}, r_{u1}), \ldots, (a_{u\text{Gu}}, d_{u\text{Gu}}, r_{u\text{Gu}})\} \quad u = 1, \ldots, U, \tag{10}$$

in which G_u denotes the total number of detections associated to hit u with the positions (a_{u1}, d_{u1}, r_{u1}) to

$(a_{u\mathrm{Gu}}, d_{u\mathrm{Gu}}, r_{u\mathrm{Gu}})$. U is used to denote the total number of plots in the current scan, whereas the sub index k has been dropped for clarity reasons.

The major advantage of CCL can be summarized in one important property: If a target is correctly detected in one or more cells by the preceding CFAR detection, this target will survive the ADMA as long as it is not merged with another target.

C. Target Parameter Estimation (TPE)

After the CCL a center of gravity (COG) algorithm [12], as one form of TPE, is applied. The algorithm estimates the azimuth centroid position $\tilde{a}_u$ of the current hit according to

$$\tilde{a}_u = \frac{\sum\limits_{\mathrm{a,d,r}\in h_u} \left(a \cdot p_{\mathrm{a,d,g}}\right)}{\sum\limits_{\mathrm{a,d,r}\in h_u} p_{\mathrm{a,d,r}}}, \tag{11}$$

in which (a,d,r $\in$ h_u) denotes all detections associated to the current hit. The term $(a \cdot p_{\mathrm{a,d,g}})$ is a product of the beam number and the power of the associated detection cell. Using a weighted estimation of beam number and power has the advantage that the estimation is more robust to asymmetrically shaped hits than simply taking the mean beam number. A typical example of such an asymmetrically shaped hit is present, if a hit is composed of target and clutter/noise detections.

Similar to the azimuth estimation the COG algorithm is also applied to the range and Doppler domain to obtain $\tilde{d}_u$ and $\tilde{r}_u$, respectively replacing a in (11) by d or r. Alternative TPE methods are enlisted in [13] and [14].

The estimated target parameters $\tilde{a}_u$, $\tilde{d}_u$ and $\tilde{r}_u$ can then be compared to reference data, for example AIS data. Using a distance measure and defining a valid detection gate surrounding the reference data makes it possible to determine if the target has been successfully detected. Utilizing the CFAR detections directly would lead to a large number of detections from each target, which would either be counted as additional targets or false alarms.

An example of the different stages of processing is illustrated in Fig. 5, consisting of the input data, the CFAR processing as well as the CCL and the COG processing, but not including the scan-by-scan averaging process.

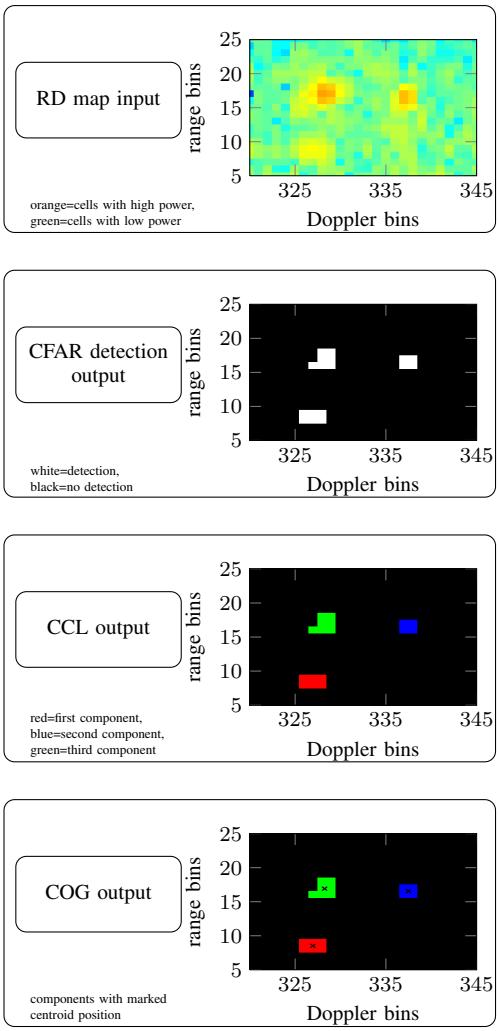

Fig. 5. Examples of different stages of proposed processing

IV. Results

The results are based on the processing of measured radar data and AIS data. The first part of this section analyzes the general performance of the proposed methods, while the second part analyzes the performance for a particular target. The preprocessed radar input data consists of 101 scans, a single beam with 220 range bins and 512 Doppler bins with properties presented in Section III-A.

For the target detection a 2D CA-CFAR algorithm, operating in the range-Doppler domain, has been chosen. To obtain comparable results, the CFAR parameters remain the same for detection on the input data as well as detection on the scan-by-scan averaged input. The number of the reference cells in range and Doppler domain are both chosen equal to four, with two guard cells surrounding the CUT in each dimension. The design false alarm rate is chosen to be equal to 10^{-3}.

Still there is one major difference for the calculation of the T factor according to (6) for the scan-by-scan averaging cases, which takes into consideration the expected higher accuracy of the estimated average noise/clutter power in the reference cells due to preceding averaging operation. Thus, in all scan-by-scan averaging cases (FIR and IIR) N is replaced by the product of original N and the number of filter tabs m of the FIR filter.

Based on the previous considerations in Section III-A the following scan-by-scan filter and parameters are chosen:

- FIR filter with $b[0] = b[1] = b[2] = 1/3$ acc. to (7)
- IIR filter with $b[0] = 2/3$, $a[1] = 1/3$ acc. to (8).

While the FIR filter performs the mean average over the current and the two past scans, the IIR filter weights the current and the past scans differently. Due to the stronger weighting of the current scan this filter is expected to have a faster response to changes.

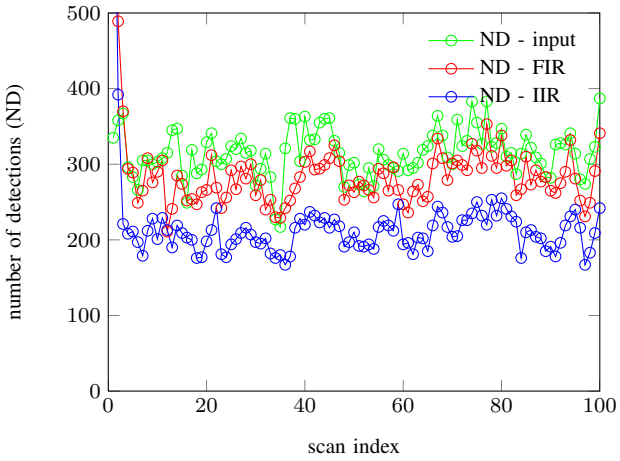

Fig. 6. Number of total detections at each scan

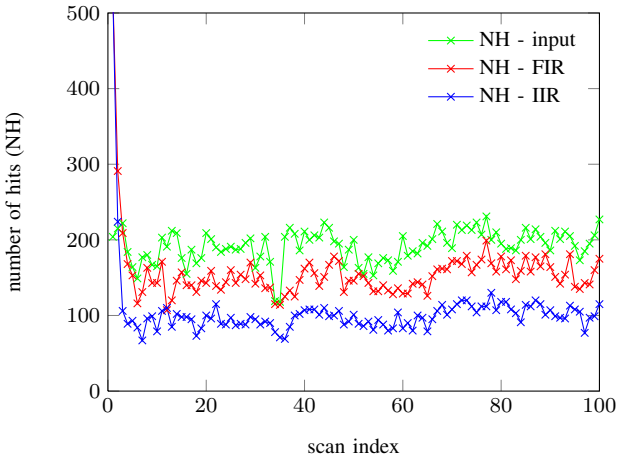

Fig. 7. Number of total hits at each scan

A. *Total number of detections and hits*

First, the influence of the SBSA operation on the total number of detections, is analyzed. The total number of detections includes true target detections, multiple detections of the same target and false alarms. In Fig. 6 the total number of CFAR detections (ND) at each scan index, based on 1.) input data, 2.) FIR averaged data and 3.) IIR averaged data, is presented.

The results show that the number of detections is reduced by applying scan-by-scan FIR filtering, but even more detections are reduced by applying scan-by-scan IIR filtering. Furthermore, it can be seen that both filters need some time to adapt. What cannot be seen in the Fig. 6 is where on the range-Doppler map the detections occur.

This has been analyzed by visual inspection of the input range-Doppler maps and shows that a significant number of detections can be attributed to false alarms in the external noise dominated regions. By analyzing the detections on the range-Doppler map of the scan-by-scan averaged data it can be seen that exactly these false detections in external noise have been significantly reduced.

At this point it should be noted that also AIS does not provide a perfect ground truth, as many smaller ships are not equipped with an AIS transmitter [15] and thus a clear distinction between correct detections and false alarms is difficult.

Another comparison of the SBSA performance can be carried out by analyzing the number of hits after the ADMA processing as illustrated in Fig. 7, with CCL using 4-connectivity and operating on 2D data. Furthermore, Fig. 7 shows that the number of hits (NH) for all three cases is approximately half of the number of detections in Fig. 6. To further analyze the assignment process of detection to hits, the average number of detections associated to each hit is illustrated in Fig. 8. It shows that for the majority of assignments a single or a double detection is mapped to one hit. This is true for all three investigated cases.

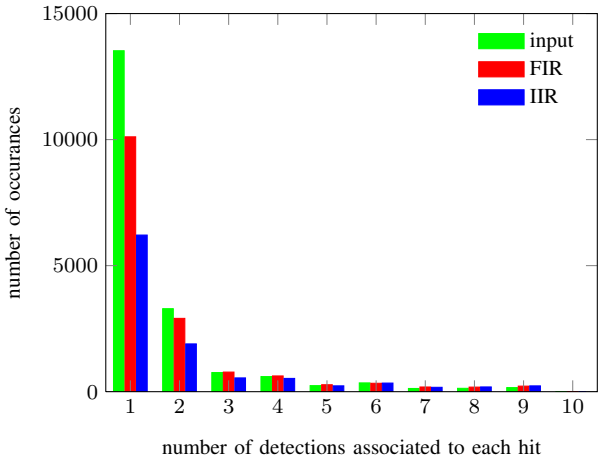

Fig. 8. Number of associated detections to each hit

B. *Analyzing the detection performance of a single target*

Besides analyzing the range-Doppler map as a whole the effect on single targets has been investigated. Of particular interest is a comparison between the power in the cell of a confirmed hit to the used CFAR threshold S to detect this target. This comparison is illustrated in Fig. 9 for all three cases (input, FIR, IIR) at each scan after carrying out CFAR, ADMA and COG processing.

We consider a confirmed hit, if the reported hit is within $\pm\Delta r$ range bins and $\pm 5 \cdot \Delta f_D$ Doppler bins of the AIS reported position. The large Doppler tolerance is needed to compensate the error due to offsets in the time of the reported position of AIS and the time of the radar measurement.

Fig. 9 shows that the impact of SBSA on the power in the target cell is small and thus no significant smearing of target power into adjacent cells occurs, even though the chosen target has a comparatively high speed of 7.5 m/s.

On the contrary, one can see that the CFAR detection threshold S of the SBSA data experiences less fluctuation than the CFAR detection threshold S of the input data. In

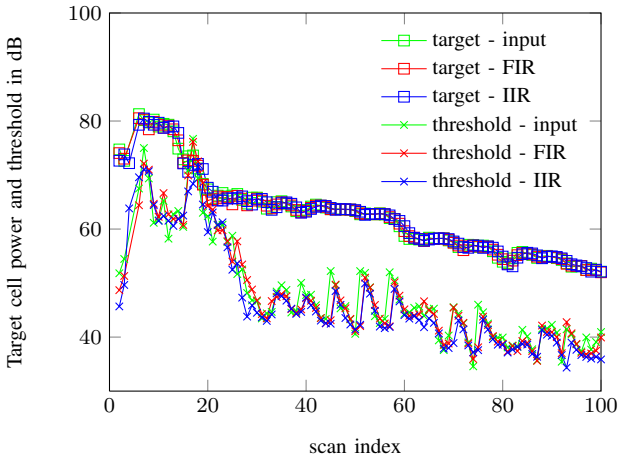

Fig. 9. Target cell power and CFAR detection threshold S at each scan

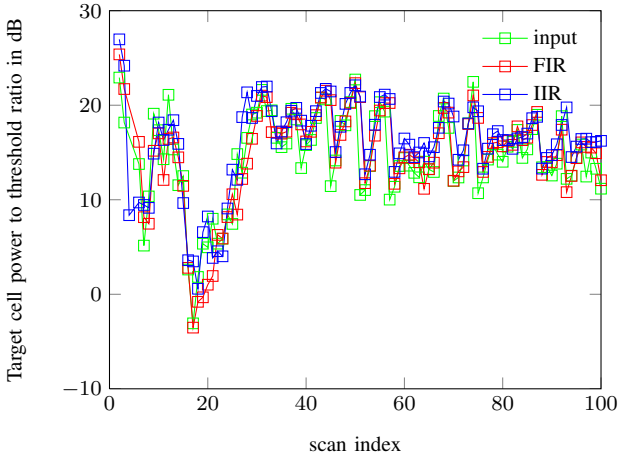

Fig. 10. Target cell power to CFAR detection threshold S ratio at each scan

addition, it can be seen that the CFAR detection thresholds S operating on the SBSA data are lower than their non-averaged counterpart.

This can be explained by the fact that the expected local estimate Z of SBSA is more accurate and concurrently a lower constant scale factor T can be used. Since successful detection is essentially a function of target cell power to CFAR detection threshold S, Fig. 10 is given, where the improvements of SBSA can be seen more clearly.

Still there are some things to keep in mind: Any filtering along different scans introduces an additional delay, so target detection can be delayed. Furthermore, an additional error in the COG estimation process for SBSA processed data can be observed. This is due to the fact that the integrated power in the associated detection bins is a mixture of several scans.

V. Conclusion

In this paper we have presented a combination of scan-by-scan averaging, ADMA and target parameter estimation in the context of HFSWR, taking into account the particular properties of ship targets and the coarse HFSWR resolution.

The approach has been evaluated on measured radar data and shows promising results to reduce the number of false alarms and a reliable way to combine several detections of the same target into one hit. The used COG algorithm shows better estimation results than simple center beam position approaches, but still offers room for improvement.

Acknowledgment

This work was supported by Wehrtechnische Dienststelle für Schiffe und Marinewaffen, Maritime Technologie und Forschung (WTD 71), Eckernförde, Germany.

The authors would like to extend their warm gratitude to Helzel Messtechnik GmbH, Germany and Dr. Dipl-Oz F. Ziemer from Helmholtz-Zentrum Geesthacht, Germany for providing the measurement data.

References

[1] D. E. Barrick, "FM/CW Radar Signals and Digital Processing," National Oceanic and Atmospheric Administration (NOAA), Tech. Rep. ERL 283-WPL 26, Jul. 1973.

[2] M. Skolnik, *Radar Handbook*, 3rd ed. New York: McGraw Hill, 2008.

[3] J. Hinz, T. Fickenscher, A. Gupta, M. Holters, and U. Zölzer, "Evaluation of time-staggered MIMO FMCW in HFSWR," in *Proceedings of the International Radar Symposium (IRS) 2011*, Sep. 2011, pp. 709–713.

[4] P. Gandhi and S. Kassam, "Analysis of CFAR processors in homogeneous background," *IEEE Transactions on Aerospace and Electronic Systems*, vol. 24, no. 4, pp. 427–445, Jul. 1988.

[5] J. Hinz, M. Holters, U. Zölzer, A. Gupta, and T. Fickenscher, "Presegmentation-based adaptive CFAR detection for HFSWR," in *IEEE Radar Conference (RadarCon) 2012*, May 2012, pp. 665–670.

[6] R. Nitzberg, "Clutter Map CFAR Analysis," *IEEE Transactions on Aerospace and Electronic Systems*, vol. AES-22, no. 4, pp. 419 –421, Jul. 1986.

[7] Z. Wang *et al.*, "Range-Doppler image processing in linear FMCW radar and FPGA based real-time implementation," *Journal of Communication and Computer*, vol. 6, no. 4, pp. 55–59, Apr. 2009.

[8] G. Trunk, "Range Resolution of Targets Using Automatic Detectors," *IEEE Transactions on Aerospace and Electronic Systems*, vol. AES-14, no. 5, pp. 750–755, Sep. 1978.

[9] A. Dzvonkovskaya, K.-W. Gurgel, H. Rohling, and T. Schlick, "Low Power High Frequency Surface Wave Radar Application for Ship Detection and Tracking," in *International Conference on Radar 2008*, Sep. 2008, pp. 627–632.

[10] F. D. Xiaojing Huang, Biyang Wen, "Ship detection and tracking using multi-frequency HFSWR," *IEICE Electronics Express*, vol. 7, no. 6, pp. 410–415, Mar. 2010.

[11] R. Sedgewick, *Algorithms in C*, 3rd ed. Amsterdam: Addison-Wesley, 1998.

[12] H. Meikle, *Modern Radar Systems*, ser. Artech House Radar Library. Artech House, 2008.

[13] H.-H. Ko, K.-W. Cheng, and H.-J. Su, "Range resolution improvement for FMCW radars," in *European Radar Conference (EuRad) 2008*, Oct. 2008, pp. 352–355.

[14] M. Bouchard, D. Gingras, Y. de Villers, and D. Potvin, "High Resolution Spectrum Estimation of FMCW Radar Signals," in *IEEE Seventh SP Workshop on Statistical Signal and Array Processing*, Jun. 1994, pp. 421–424.

[15] S. Maresca, J. Horstmann, R. Grasso, M. Coffin, K.-W. Gurgel, and T. Schlick, "Performance assessment of HF-radar ship detection," in *Proceedings of the International Radar Symposium (IRS) 2011*, Sep. 2011, pp. 131 –136.